

### **33a-L.0 IN-SITU STUDIES OF STRAIN RATE EFFECTS ON PHASE TRANSFORMATIONS AND MICROSTRUCTURAL EVOLUTION IN BETA-TITANIUM ALLOYS (LEVERAGED)**

Benjamin Ellyson (CSM)

Faculty: Amy Clarke (CSM)

Other Participants: Yaofeng Guo (CSM)

Industrial Mentor: Austin Mann (Boeing), TBD (AFRL)

#### **33a.1 Project Overview and Industrial Relevance**

Titanium alloys are heavily used in the aerospace and biomedical industries for their high specific strength and good corrosion resistance. However, low work hardening and uniform elongation have limited their applicability in deformation controlled applications, where high absorbed energy or high formability are required. The ability to develop novel titanium alloys that exhibit high work hardening would broaden their applicability, such as lightweight blast-resistant armor, crash resistant structural components and high-complexity plastically formed parts. Recent work [33.1-33.4] on metastable  $\beta$ -titanium alloys has shown promising results, wherein high work hardening and uniform elongations were achieved through transformation induced plasticity (TRIP) and twinning induced plasticity (TWIP). These deformation mechanisms have been the subject of extensive study in ferrous alloys, while published work in other alloy systems, such as BCC titanium in particular, is limited in scope. The present project aims to study TRIP and TWIP effects in  $\beta$ -titanium to garner fundamental understanding of the intrinsic and extrinsic variables controlling TRIP and TWIP. The fundamental knowledge gained from this study will be used to develop an alloy design methodology that will enable the tailoring of microstructural evolution, deformation mechanisms, and mechanical response by means of alloying and processing.

#### **33a.2 Previous Work**

Initial characterization and compression tests were performed on solution treated Ti-1023 stock, as previously reported. Solution treatments were performed, as indicated in Table 33.1, and the initial microstructure for each condition was characterized by optical microscopy (OM). Evaluation of work-hardening was performed to screen for potential TRIP/TWIP behavior. The original intent was to identify best-case conditions for further mechanical testing and post-mortem characterization.

#### **33a.3 Recent Progress**

##### **33a.3.1 Microstructural Characterization**

Since the last reporting cycle, further refinement of solution treatment and sample preparation procedures have allowed for the production of a fully retained, equiaxed  $\beta$  structure. Grain sizes ranging from roughly 200 to 1200  $\mu\text{m}$  have been produced by varying solution temperatures from 800 to 1200  $^{\circ}\text{C}$  and hold times varying from 0.5h to 3h. Almost all samples discussed or presented since the last reporting cycle have been shown to be free of athermal martensite after solution treatment.

OM and scanning electron microscopy (SEM) investigations of solution treated samples have shown chemically homogeneous microstructures; the only measurable difference between different solution treatment temperatures is grain size, resulting from the different solution hold times and temperature. Further transmission electron microscopy (TEM) investigations are required to quantify the effect of solution temperature and hold time on athermal  $\omega$  phase fraction. However, initial results indicate that all the treatments explored here produced a fine, uniform dispersion of spherical  $\omega$  particles at the nanometer scale.

##### **33a.3.2 Compression Testing**

The compression study on Ti-1023 was completed shortly after the last reporting cycle. Post-mortem microstructural characterization revealed conclusively that microstructural evolution occurred for every solution treatment investigated after deformation. OM revealed the presence of lath-like deformation products in each condition, although the nature of the product could not be identified by OM. Mechanical testing data (stress-strain and work

hardening behavior) did not show consistent evidence of TRIP/TWIP, as initially thought. Additional testing was performed in triplicate to obtain statistics (mean and standard deviation) to clarify the behavior. The conclusions presented herein are from the helium quenched (HQ) condition, but negligible differences were found for the water quenched (WQ) condition. Figure 33.2 presents the average work hardening rate for three solution treatments (HQ) and the as-received (AR) state. The average work hardening was calculated as the average value of the instantaneous work-hardening rate from 0.5% strain after yield up to a final strain of 8%. The average work hardening rate decreases with increasing solution temperature. This is thought to be due to increasing grain size, which leads to a lower density of nucleation sites and an overall lower barrier to transformation/propagation of the product. This yields a lower density of coarser product, which in turn implies less interface in the material to impede slip and increase work hardening.

However, the compression study did not yield a clear trend for the effect of solution treatment temperature on yield stress. The scatter of available data was too large for any conclusive trend to be identified, although a weak positive correlation may exist.

### **33a.3.3 Initial Tensile Testing**

An experimental plan for the tensile study was devised to understand the effect of grain size on the work hardening behavior and uniform elongation in Ti-1023. It is well known that compression tests cannot be used to evaluate uniform elongation of a material and need to be corrected to eliminate experimental contributions to work hardening behavior, such that tensile testing is preferred for a quantitative evaluation of these material parameters. Secondly, as indicated in section 33.a.3.1, only grain size varied between the heat treatments (the effect of heat treatments on athermal  $\omega$  phase dispersion is still to be determined), such that the experimental matrix for the tensile study was devised to control grain size, while keeping other parameters constant. The heat treatment schedule is shown in Table 33.2. The initial and final treatments are the same for all samples, producing equivalent final microstructures consisting of fully equiaxed  $\beta$  and athermal  $\omega$ , while certain samples (designated as “large-grained”) will undergo an intermittent grain-growth solution treatment to produce much larger grains.

Initial testing was completed on a small set of tensile specimens to validate the proposed experimental plan. Samples of all three conditions ( $\alpha/\beta$  produced by the 700°C-1h treatment, small grained fully  $\beta$  produced by the 850°C -1h treatment and large grained fully  $\beta$  produced by the 1100°C -3h treatment) were tested to various increments of strain, up to failure. Figure 33.3 presents the true stress-true strain plots of the three tested conditions, clearly showing a difference in behavior among the large and small grained fully  $\beta$  specimens (1100°C -3h and 850°C -1h, respectively), and an even larger difference between both  $\beta$  samples and the  $\alpha/\beta$  state (700°C -1h), which represents a fully chemically stable  $\beta$  matrix as it does not exhibit TRIP/TWIP effects. Interestingly, only one other study has been published on the effect of grain size on the TRIP effect in Ti-1023. In their work, Battacharjee et al. [33.5] concluded that increasing  $\beta$  grain size lead to diminishing TRIP, until a maximum grain size of roughly 800  $\mu\text{m}$ , where it disappeared completely. However, our initial results indicate the contrary, as the large-grained sample (1100°C -3h) clearly shows signs of TRIP-enhanced work hardening at an average grain size of approximately 1200  $\mu\text{m}$ . These novel results will be examined in greater detail in upcoming work.

### **33a.4 Plans for Next Reporting Period**

By the next reporting period, quasi-static tensile testing of Ti-1023 at multiple strain rates and grain sizes will be completed and analyzed. Fine-scale microstructural characterization is also planned by interrupted tensile testing to characterize microstructural evolution and deformation product as a function of strain during the early stages of deformation (0.5% to 2% plastic strain). Higher rate and in situ tensile testing is also planned to gain understanding of TRIP/TWIP and slip during deformation. A Ti-15 wt% Mo alloy was recently received from ATI. It is currently being characterized and will be used for quasi-static and dynamic testing in the future.

In summary, the following work is planned in the upcoming months:

- A beam-time request was submitted to APS for 2019. Proposed experiments include high-strain rate imaging and diffraction of Ti-1023 and Ti-15Mo in a Kolsky bar setup. Kolsky bar tests of Ti-1023 and Ti-15Mo are also planned at LANL for post-mortem characterization.
- Tensile testing of Ti-1023 will be completed (Table 33.2);.
- Strain rate effects on TRIP/TWIP of Ti-1023 in tension will be performed.
- A heat-treatment matrix will be developed for the Ti-15Mo alloy provided by ATI to identify microstructural evolution during initial compression testing.

### 33a.5 References

[33.1] C. Brozek, et al., A  $\beta$ -titanium alloy with extra high strain-hardening rate: design and mechanical properties, *Scripta Materialia* 114 (2016): 60-64.

[33.2] F. Sun, et al. A new titanium alloy with a combination of high strength, high strain hardening and improved ductility, *Scripta Materialia* 94 (2015): 17-20.

[33.3] M. Marteleur, et al., On the design of new  $\beta$ -metastable titanium alloys with improved work hardening rate thanks to simultaneous TRIP and TWIP effects, *Scripta Materialia* ,10 (2012): 749-752.

[33.4] X. Min, et al., Mechanism of twinning-induced plasticity in  $\beta$ -type Ti-15Mo alloy, *Scripta Materialia* 69.5 (2013): 393-396.

[33.5] A. Bhattacharjee, et al., Effect of  $\beta$  grain size on stress induced martensitic transformation in  $\beta$  solution treated Ti-10V-2Fe-3Al alloy, *Scripta materialia* 53.2 (2005): 195-200.

### 33a.6 Figures and Tables

Table 33.1 Initial heat treatment schedule investigated for Ti-1023

Temperature (°C)	Time (h)	Quench
900	2	Water or Helium
1000	2	Water or Helium
1100	2	Water or Helium
1200	2	Water or Helium

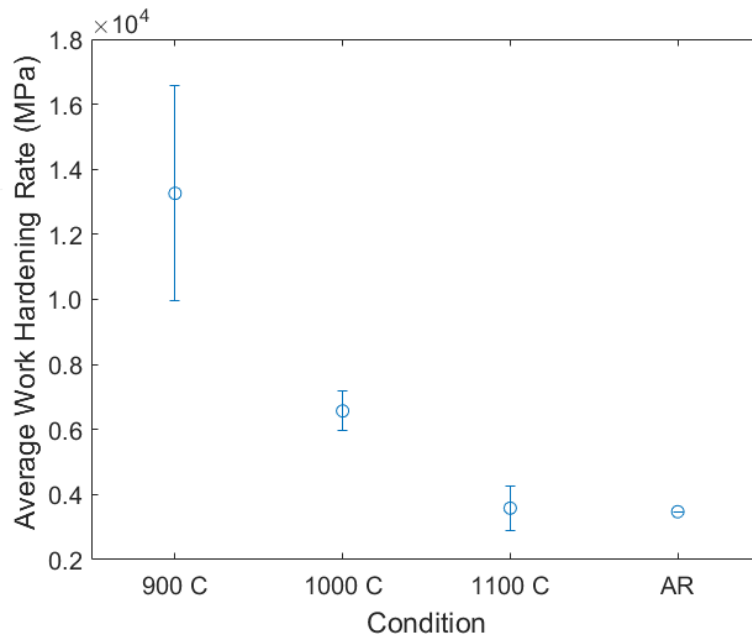


Figure 33.2 Average instantaneous work hardening rate with error bars as a function of solution treatment temperature and the As-Received (AR) state. Note the clear negative trend as temperature increases (correlated to grain size). The three solution treated states are helium quenched samples.

Table 33.2 Heat treatment schedule for tensile study of Ti-1023

Temperature (°C)	Time (h)	Quench	Comment
700	1	Water	$\alpha/\beta$ homogenizing step
1100	3	Water	Optional grain growth step for large grain samples
850	1	Water	Homogenizing solution treatment (athermal $\omega$ phase)

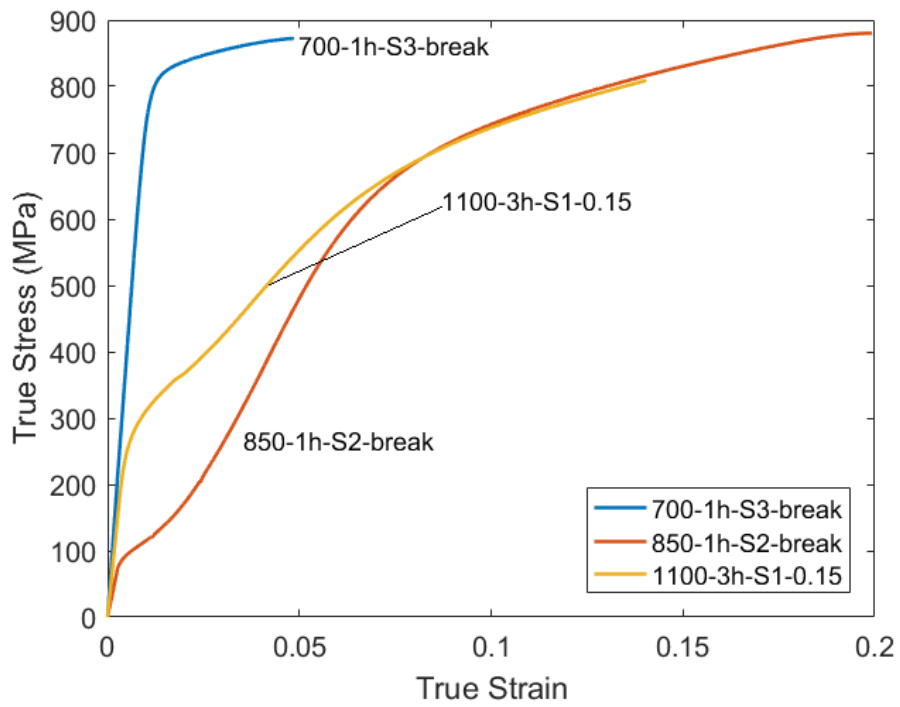


Figure 33.3 True stress-strain curves for the three different steps of the heat treatment procedure. Note the clear difference in yield stress (YS) and work hardening rate between the  $\alpha/\beta$  700°C state and both fully  $\beta$  states (850°C and 1100°C).